Estuarine, Coastal and Shelf Science (1998) **46,** 333–350

Estimation of Dispersion and Characteristic Mixing Times in Plum Island Sound Estuary

J. J. Vallino and C. S. Hopkinson, Jr.

The Ecosystems Center, Marine Biological Laboratory, Woods Hole, MA 02543, U.S.A.

Received 4 October 1996 and accepted in revised form 4 August 1997

Salinity distributions, dye release studies, and parameter estimation techniques are used to determine the longitudinal (or tidal) dispersion coefficient in the Plum Island Sound estuary in north-eastern Massachusetts, U.S.A. A one-dimensional, intertidal, advection–dispersion model is used to test the validity of the steady-state assumption employed to estimate tidal dispersion from salinity. It is found that salinity distributions in the upper Parker River can take months to relax to steady state under low freshwater discharge conditions, so that dispersion cannot be reliably estimated using the steady-state assumption. To overcome this problem, dye release studies and parameter estimation techniques are used to determine the functionality of the dispersion coefficient that produces the best fit between the observed salinity profiles, dye plumes and model output under transient conditions for the period between 28 April 1992 and 12 April 1995. The estimated dispersion coefficient is found to be a hyperbolic function of distance from the head of the estuary and varies from an average of 3·6 $m^2 s^{-1}$ in the upper Parker River (0–5·2 km) to an average of 670 $m^2 s^{-1}$ in Plum Island Sound (14·3–24 km). The advection–dispersion model is also used to investigate three characteristic mixing-time scales involving average age, average residence time and average transit time (also called turnover or flushing time) for freshwater and saltwater sources in defined subsections of the estuary. It is found that these time scales can vary from a few hours to 3 months depending on location and freshwater discharge. Transport in the upper Parker River can be either advection or dispersion dominated depending on discharge, while Plum Island Sound is always dominated by dispersive terms. Tidal channel morphometry leads to a very dynamic system in the upper Parker River that significantly impacts ecological processes in the region. We discuss the relevance and appropriate application of the three characteristic mixing-time scales to ecological processes.

Keywords: dispersion; average age; average residence time; average transit time; Massachusetts coast

Introduction

Mixing processes have a major impact on the biology, chemistry, ecology and water quality of estuarine environments. While much observational and theoretical research has focused on identification and quantification of the physical mechanisms driving mixing and dispersion (Ketchum, 1951; Fischer, 1976; Zimmerman, 1976; Chatwin & Allen, 1985), little progress has been made on predicting dispersion from first principles (but see Smith, 1977). This is largely due to the extreme complexity of estuarine systems including great variation in geometry and bathymetry, density structure, wind stress, freshwater input and tidal forcing. Variation occurs not only between estuaries but also within estuaries, both with respect to space and time.

High-resolution two- and three-dimensional primitive equation models are capable of resolving many of the mixing processes (Blumberg & Kantha, 1985; Dortch *et al.*, 1992; Blumberg *et al.*, 1993). However, such models are computationally intensive and require a significant investment of resources to implement for a particular estuary, especially if coupled with complex biogeochemical and food-web models. Consequently, mixing phenomena in estuaries that have not been extensively studied are often approximated by a single longitudinal dispersion coefficient (also called tidal dispersion), which is analogous to Fickian diffusion in that transport is assumed to be proportional to a concentration gradient (Dronkers, 1982; Guymer & West, 1992). The tidal dispersion coefficient (which we will refer to as dispersion henceforth) includes mixing not only due to diffusive transport, but advective transport as well, such as vertical and lateral shear dispersion, and tidal trapping and pumping (Dortch *et al.*, 1992; Geyer & Signell, 1992; Guymer & West, 1992). The use of a dispersion coefficient greatly simplifies the modeling effort that is required to capture the general transport of nutrients and plankton, and the residence time of pollutants in an estuary. Since the dispersion coefficient, $D(x,t)$, is used as a macroscopic quantity to capture large-scale mixing processes that occur over

0272–7714/98/030333+18 $25.00/0/ec970281

broad spatial scales, its accurate estimation is critical to capturing transport phenomena in an estuary.

The dispersion coefficient is highly dependent on many factors that are unique to individual estuaries. It varies over space and time in response to changes in channel morphometry, freshwater discharge, tidal currents and wind stress (Fischer *et al.*, 1979). To estimate the dispersion coefficient in a particular estuary, one of three possible approaches is employed typically. Most commonly, the dispersion required to maintain an observed conservative tracer (e.g. salt) distribution along the length of an estuary is calculated, assuming the distribution is at steady state (Officer, 1978). Dye studies where the release and subsequent dispersion of the dye are monitored over several tidal cycles is another approach (Hetling & O'Connell, 1966; Gunn & Yenigun, 1985). The third approach, not used in this study, is to measure deviations in velocity and salinity from their spatial means (Dyer, 1974; Park & James, 1989; Guymer & West, 1992). Dye studies have the advantage of not being dependent on the steady-state assumption and of providing high-resolution estimates of dispersion in regions of minimal horizontal salt gradients (i.e. where application of the first approach is difficult). However, they do not generally provide a synoptic view of dispersion over the entire length of the estuary due to constraints on the amount of dye that can be released.

In this paper, both dye and salt distribution techniques were utilized to examine the dispersion coefficient in the Plum Island Sound estuary in Massachusetts. In this shallow, macrotidal estuary, longitudinal dispersion is the focus of attention. The analysis is coupled to a one-dimensional, intertidal, advection–dispersion model to investigate the validity of the steady-state assumption in this estuary. Three different characteristic mixing-time scales in various reaches of the estuary were examined, and the relevance of these time scales to the ecology and water quality of the system is discussed.

Site description

The study was conducted in the Plum Island Sound estuary in north-eastern Massachusetts, U.S.A. (Figure 1). The estuary and its watersheds lie within the Seaboard Lowland section of the New England physiographic province (Fenneman, 1938). The rivers and estuary discharge into the Gulf of Maine, a semi-enclosed sea off the Atlantic Ocean. The Gulf of Maine coastal-current flows to the south along the coast. Coastal salinity varies seasonally in relation to land runoff and has a major influence on Plum Island Sound salinity (Blumberg *et al.*, 1993).

The Plum Island Sound estuary is a coastal-plain estuary with extensive areas of productive, tidal marshes. The 24 km long bar-built estuary is well mixed with a type 1A circulation regime (Hansen & Rattray, 1966). Tides are semi-diurnal with an average tidal range of 2·9 m and a spring–neap range of 2·6–3·6 m. Marshes flood only during spring tides. Estimated tidal prism is about 32 Mm^3. Mean depth increases along the length of the estuary from about 1·4 m at the head of the estuary to about 5·7 m 11 km downstream at the head of the sound. Depths then increase through the broad shallow sound to about 1·8 m prior to increasing to about 4·7 m at the mouth of the estuary. Water-body area ranges from 7·2 to 14·9 km^2 from low to high tide. There are extensive areas of non-vegetated, intertidal flats at low tide. In this estuary where the typical spacing of topographic features is considerably less than the tidal excursion and tidal amplitude is of the same order as average depth, tidal shear dispersion is probably the primary mechanism contributing to mixing (Smith, 1977; Geyer & Signell, 1992). Annual water temperature range is from $-1{\cdot}0$ to 28 °C and salinity range is from 0 to 32. Vegetation is typical of New England marshes, the major wetland species being *Spartina alterniflora* and *S. patens* in brackish and saline regions, and *Typha*, *Scirpus* and *Carex* in freshwater regions.

The 608·9 km^2 watershed draining into the estuary has two major rivers, the Parker and Ipswich Rivers, and eight secondary creeks. Locations of runoff inputs are identified in Figure 1. The USGS monitors discharge for 55·2 and 328·8 km^2 portions of the Parker and Ipswich Rivers, respectively. Discharges from ungauged portions of the watershed are estimated from area:discharge relations calculated for the gauged portion of the Parker River. Average annual discharge for the Parker River is 1·0 $m^3\,s^{-1}$, ranging seasonally from 0·2 $m^3\,s^{-1}$ in summer to 2·4 $m^3\,s^{-1}$ in winter. Calculated average annual discharge for the entire watershed draining into the estuary is 11·0 $m^3\,s^{-1}$. Discharge is thus about 67 times lower in volume than a single tidal prism. Precipitation is evenly distributed throughout the year and averages 112 cm $year^{-1}$, 44% of which is returned to the atmosphere via evapotranspiration (Sammel, 1967). Air temperature fluctuates annually between an average winter minimum of -7 °C and an average summer maximum of about 28 °C (Sammel, 1967).

Based largely on estuarine metabolic patterns and tidal excursion lengths, we have identified four regions of interest in the estuary: upper (0–5·2 km, high tide volume 0·58 Mm^3), mid (5·2–9·3 km, 1·5 Mm^3), and lower (9·3–14·3 km, 4·8 Mm^3) portions of the Parker River and the sound (14·3–24 km, 33 Mm^3,

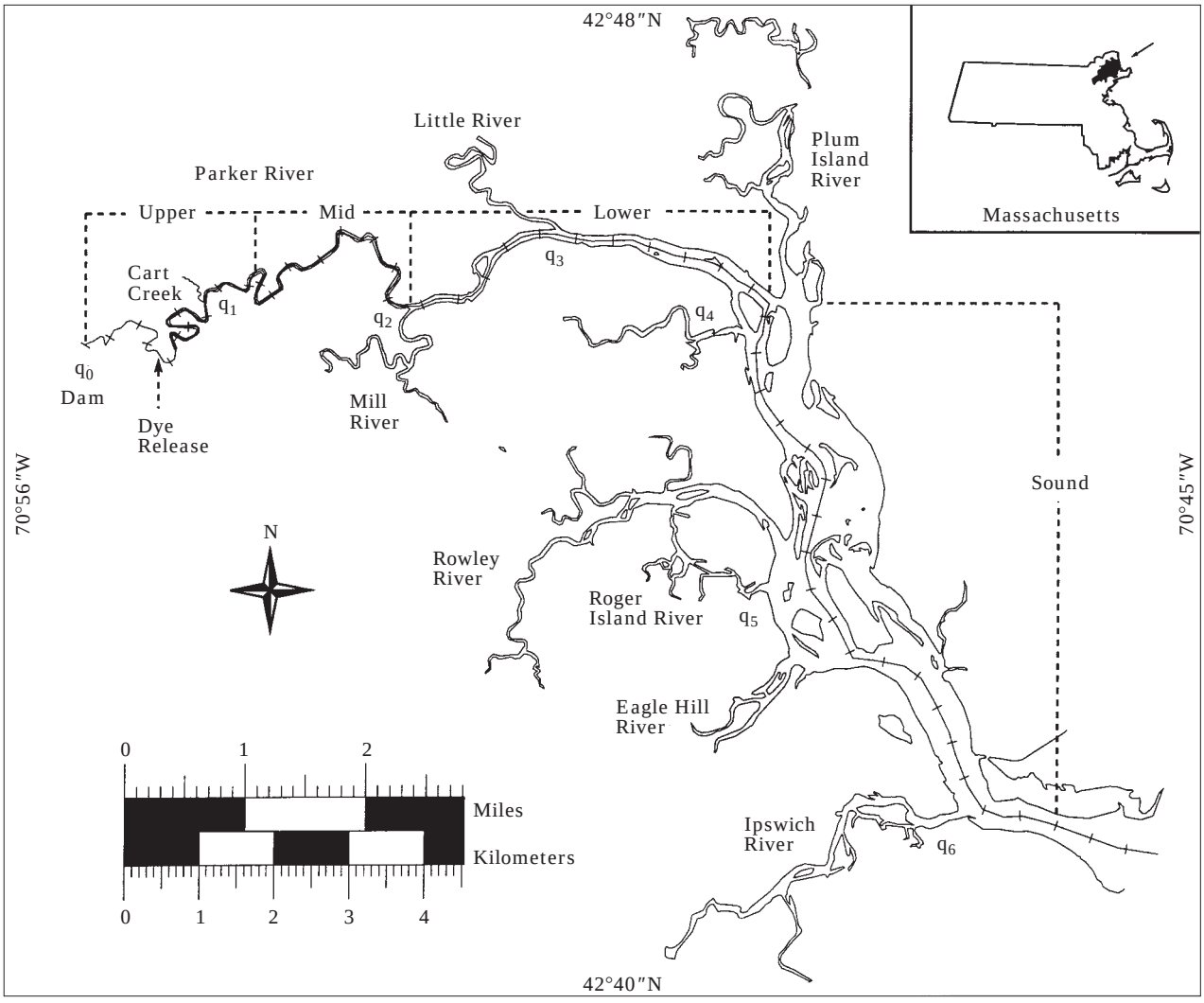

FIGURE 1. Map of Plum Island Sound estuary in north-eastern Massachusetts, U.S.A. based on MassGIS data. Hatch marks along approximate center line of Parker River and sound are spaced 0·5 km apart starting at the dam. Dotted lines delineate the four subsections of the estuary reference in the main text, and the dotted arrow indicates the location of the two dye release studies. Approximate locations of the seven lateral inputs associated with Equation 4 and Table 1 are marked as q.

Figure 1). Average tidal excursion at the mid-point of these regions is approximately 4, 6, 14 and greater than 14 km, respectively.

Field observations

Salinity at selected locations along the Parker River and Plum Island Sound (Figure 1) was calculated (Miller *et al.*, 1988) from conductivity measurements taken with a Hydrolab H20 probe (Hydrolab Corp.), except for data reported on 28 April 1992, 26 August 1992, 25 September 1992, 16 December 1992, 3 June 1993, 7 July 1993, and 2 December 1993, which were obtained from Rines *et al.* (1994). Since depth and lateral profiles of salinity exhibited little deviations, all salinity measurements were taken at one point from the surface at high tide and assumed to be indicative of cross-sectional averages.

Two dye plume experiments were conducted under extreme low (0·008 $m^3 s^{-1}$ on 4–6 August 1993) and average (0·8 $m^3 s^{-1}$ on 10–13 April 1995) Parker River discharge regimes. Point releases of Rodamine Wt fluorescent dye (Formulabs, Inc.) of 1·6 l (in 1993 experiment) and 7·7 l (in 1995 experiment) were made in the upper Parker River (at about 1·7 km) at high tide and well mixed over the river cross-section. On subsequent high tides, the dye concentration as a function of distance along the river was measured with a Turner Designs Model 10-AU Fluorometer

equipped with a Rodamine dye filter set, a 25 mm flow-through optical cell, and a temperature compensation probe. Initial vertical and lateral profiles of the dye showed complete mixing over the river's cross-section after less than one tidal cycle. Surface-water samples were collected under way by employing a ram tube which forced surface water through the fluorometer flow cell as well as a flow cell attached to the Hydrolab probe. We measured dye fluorescence, conductivity, temperature and dissolved oxygen. This sampling technique provided nearly synoptic high tide measurements of the dye plume and water properties since it allowed travel at the speed of the tidal wave.

Upper and mid Parker River (0–12 km) cross-sectional areas were determined from high-tide depth profiles taken at four equally spaced points across the river with a depth finder (Hummingbird). Cross-sectional areas for the lower Parker River and sound (12–24 km) were determined from NOAA map 13282 (Newburyport Harbor and Plum Island Sound, 9th ed., 23 March 1991).

Modeling

In order to synthesize field observations and calculate characteristic mixing-time scales, a one-dimensional, intertidal, advection–dispersion transport model was used to simulate the distribution of salt and tracers averaged over a cross-section at high tide, $\mathbf{c}(x,t)$, as a function of longitudinal distance, x, and time, t, in the estuary (Fischer, 1976; Vörösmarty & Loder, 1994; Hopkinson, Jr. & Vallino, 1995):

$$-\frac{x_c A(x)}{V_c}\frac{\partial \mathbf{c}'(x,t)}{\partial t'} = \frac{\partial}{\partial x'}\left(-\frac{D(x,t)A(x)}{x_c q_c}\frac{\partial \mathbf{c}'(x,t)}{\partial x'} + \frac{q(x,t)}{q_c}\mathbf{c}'(x,t)\right) - \frac{x_c \mathbf{c}_c^{-1}}{q_c}\left(A(x)\mathbf{r}(x,t) + \sum_{i=0}^{n}\left(\frac{\mathbf{c}_{li}(t)}{x_c}\frac{\partial q_i(x,t)}{\partial x'}\right)\right) \quad (1)$$

This equation results from a simple one-dimensional mass balance around a point x in the estuary. The first two terms on the right-hand side of Equation 1 account for dispersive and advective transport, respectively. The third term accounts for production of material by chemical processes, where $\mathbf{r}(x,t)$ is the source term (mole m^{-3} day^{-1}), and the fourth term accounts for material associated with lateral inputs, where $\mathbf{c}_{li}(t)$ is a vector containing the concentration of the state variables in lateral input i. The equation has been placed in non-dimensional form (indicated by the prime notation) by the following transformations:

$$t = \frac{V_c}{q_c}t', \quad x = x_c x', \quad \mathbf{c}(x,t) = \mathbf{c}_c \mathbf{c}'(x,t) \quad (2)$$

where V_c, q_c, and x_c are the characteristic volume (m^3), river discharge (m^3 day^{-1}), and distance (m), respectively, and $\mathbf{c}_c$ is a diagonal matrix of characteristic concentrations of the state variables (mass m^{-3}). The river cross-sectional area at high tide, $A(x)$, is given by the following simple polynomial (m^2):

$$A(x) = a_0 + a_1 x + a_3 x^3 \quad (3)$$

which was fit to the area data collected for the Plum Island Sound estuary (Table 2). The volumetric flow-rate, $q(x,t)$, is a function of both time and distance along the estuary. The spatial component of $q(x,t)$ is used to capture lateral inputs from tributaries that contribute to the total longitudinal flow in the estuary, and is described by (m^3 day^{-1}),

$$q(x,t) = \sum_{i=0}^{n} q_i(x,t),$$

$$\text{where} \qquad q_i(x,t) = \left(\frac{W_i}{W_{PR}}\right)\frac{q_{PR}(t)}{(1+e^{-\sigma(x-x_i)})} \quad (4)$$

$q_{PR}(t)$ is the USGS gauged Parker River discharge at Byfield, Massachusetts, U.S.A., W_{PR} is the watershed area of the gauged Parker River, W_i is the sub-watershed area (Rines *et al.*, 1994) of lateral input i (Figure 1, Table 1), x_i is the location of lateral input i, and σ governs the distance over which a lateral input is spread longitudinally. The total discharge associated with lateral input i is given by:

$$q_i(t) = \int_{-\infty}^{\infty}\frac{\partial q_i(x,t)}{\partial x}dx = \frac{W_i}{W_{PR}}q_{PR}(t) \quad (5)$$

and the total material transported to the estuary by lateral input i is given by $\mathbf{c}_{li}(t)q_i(t)$. The production term, $\mathbf{r}(x,t)$, for salt is $r_s(x,t)=0$, which is conserved, while Rodamine dye is assumed to be lost by first-order decay as given by, $r_d(x,t) = -k_d c_d(x,t)$, where k_d is the decay constant (Hetling & O'Connell, 1966).

We note that Equation 1, and supporting equations, should be regarded as ' model ' subject to verification in the estuary of interest (Fischer *et al.*, 1979; Chatwin & Allen, 1985). Many assumptions are embodied in Equation 1, most notably that mixing caused by Stokes' drift and the resulting compensation flow can be represented as a one-dimensional diffusive process (Dyer, 1974; Fischer *et al.*, 1979; Dortch *et al.*, 1992). In estuaries where the tidal amplitude is of the same order as average depth (such as in Plum Island Sound estuary), non-linearities between tidal wave height

TABLE 1. Locations and watershed area for lateral inputs

Input source	Label $q_i(x,t)$	Location (km)	Watershed area W_i (km^2)	W_i/W_{PR}
Parker dam	q_0	0	65·2	1·18
Cart Creek	q_1	4·2	13·5	0·245
Mill River	q_2	9·3	48·3	0·875
Little River	q_3	11·7	27·2	0·493
Mud Creek and Plum Island River	q_4	15·1	9·3	0·169
Rowley, Roger Island and Eagle Hill Rivers	q_5	19	42·4	0·768
Ipswich River	q_6	22·9	403	7·30

Sub watershed areas are based on Rines *et al.* (1994), where W_{PR} is the watershed area (55·2 km^2) for the USGS gauged Parker River discharge at Byfield, Massachusetts, U.S.A.

TABLE 2. Parameter values used for the one-dimensional advection–dispersion equation (Equation 1)

Parameter	Value	Units
V_c	1×10^6	m^3
q_c	86 400[a]	m^3 day^{-1}
x_c	24 000	m
x_L	0	m
x_R	24 000	m
a_0	45	m^2
a_1	0·02	m
a_3	4×10^{-10}	m^{-1}
σ	0·005	m^{-1}
k_d	0·14	day^{-1}

[a]Value adjusted to actual flow-rate for characteristic time scale studies.

and tidal currents can induce a substantial landward residual current (Stokes' drift) and a seaward mass-compensating residual current that are both typically much larger than the mean residual current [i.e. $q(x,t)/A(x)$] (Longuet-Higgins, 1969; Dyer, 1974; Feng *et al.*, 1986*a*; Dortch *et al.*, 1992). In macrotidal systems, these tidally induced shear flows combined with vertical or horizontal eddy diffusivity are the dominant mixing processes in the estuary (Smith, 1977; Geyer & Signell, 1992). Since such two- or three-dimensional mixing processes cannot be explicitly represented in a one-dimensional model (Chatwin & Allen, 1985; Feng *et al.*, 1986*b*), it is common practice to approximate advective transport resulting from tidal forcing by a Fickian-type diffusion, $D(x,t)\partial\mathbf{c}(x,t)/\partial t$, where $D(x,t)$ is known as the longitudinal (or tidal) dispersion coefficient (Dortch *et al.*, 1992; Guymer & West, 1992). Indeed, longitudinal dispersion is the result of the spatial averaging required to derive the one-dimensional model (Guymer & West, 1992). The validity of the approximation cannot be easily determined *a priori* and is best verified by comparing model predictions to observations of salinity distributions and tracer transport. However, the approximation seems well justified for the Plum Island Sound estuary, especially for the Parker River due to its narrow dimensions (Smith, 1977; Dronkers, 1982) which results in rapid lateral mixing.

Due to the approximations invoked to derive Equation 1, the functionality and magnitude of the tidal dispersion coefficient ($D(x,t)$, m^2 day^{-1}) is not well known and must be determined experimentally if a realistic representation of the transport of material in the estuary is to be obtained. The following three techniques were employed to estimate $D(x,t)$. First, $D(x,t)$ was estimated from salinity profiles under the assumption that the system is at steady state (Dyer, 1974; Officer, 1978), so that Equation 1 reduces to (in dimensional form):

$$D(x) = \frac{q(x)c_s(x)}{\frac{dc_s(x)}{dx}A(x)} \tag{6}$$

In order to improve the estimate of the salinity gradient, $dc_s(x)/dx$, a three parameter sigmoidal function:

$$c_s(x) = \frac{a}{1 + e^{-b(x-c)}} \tag{7}$$

was first fitted to the salinity data, and the derivative of this function at the locations where salinity was measured was calculated. This fitting procedure reduces errors introduced by the quasi-synoptic sampling technique.

Although the steady-state approximation is often used to estimate $D(x,t)$, it can not be employed reliably in those parts of the estuary where the

longitudinal salinity gradient, $dc_s(x)/dx$, is near zero and/or when the system has not attained steady-state operation, which is often true during low freshwater discharge. Consequently, the second method used to estimate $D(x,t)$ in the upper Parker River was obtained from dye tracer studies in which a one-dimensional Gaussian function for dye concentration (ppb) (Fischer *et al.*, 1979),

$$c_d(x,t) = \frac{V e^{-k_d t}}{A(x)\sqrt{4\pi D(x,t)\,t}} \exp\left[-\frac{(x-x_p)^2}{4D(x,t)\,t}\right] \times 10^9 \quad (8)$$

was fit to the dye plume distribution at each tidal cycle for which the dye was measured. Although this function is the solution to the dispersion equation for a dye release of volume V at location x_p in a system with infinite boundaries and no advection, it was found to fit the experimental data quite well if x_p was allowed to drift with the mean flow.

The third technique to improve the estimate of the dispersion coefficient was obtained by tuning parameters of a function that governs $D(x,t)$ so as to minimize the squared error between the observed, $\bar{c}_s(x_j,t_i)$, and predicted, $\hat{c}_s(x_j,t_i)$, salinity profiles from Equation 1 at each sample point x_j and time t_i, and between the predicted dispersion at the dye release site, $\hat{D}(x_{dye},t)$, and the observed dye dispersion, $\bar{D}_{dye}$. The conjugate gradient routine PRAXIS (Brent, 1973) (available via netlib at URL http://www.netlib.org/) was used to find the minimum of the cost function:

$$\mathcal{J} = \sum_i \sum_j (\bar{c}_s(x_j,t_i) - \hat{c}_s(x_j,t_i))^2 + (\hat{D}(x_{dye},t) - \bar{D}_{dye})^2 \quad (9)$$

with respect to the parameters governing the function of $D(x,t)$. To prevent numerical integration problems, a $\sin^2$ transform (Box, 1966) was used to place upper and lower bounds on the searchable parameter space.

Boundary conditions and implementation

Since the freshwater input to the Parker River flows over a dam, the left boundary condition (up-estuary, $x = x_L$) for Equation 1 is specified as a time varying flux, given by:

$$\left[-\frac{A(x)D(x,t)}{q_c x_c}\frac{\partial \mathbf{c}'(x,t)}{\partial x'} + \frac{q(x,t)}{q_c}\mathbf{c}'(x,t)\right]_{x=x_L} = \mathbf{c}_c^{-1}\mathbf{c}_L(t)\left.\frac{q(x,t)}{q_c}\right|_{x=x_L} \quad (10)$$

where $\mathbf{c}_L(t)$ is the concentration of the state variables in the river input at time t. The right boundary condition (down-estuary, $x = x_R$) specific the time varying concentration of the state variables at the mouth of the sound, and is given by:

$$\mathbf{c}'(x,t)|_{x=x_R} = \mathbf{c}_c^{-1}\mathbf{c}_R(t) \quad (11)$$

where $\mathbf{c}_R(t)$ is the concentration of the state variables in the mouth of the sound, or just offshore.

For the salt balance, $c_{Ls}(t)$ is set to zero (freshwater input), while $c_{Rs}(t)$ is set by salinity measured in the mouth of the sound during each transect and is interpolated between measurements (Figure 2). Variations in salinity at the estuarine mouth with time are probably influenced more by the Merrimac River and other large rivers in the Gulf of Maine, than by the Parker River and associated lateral inputs (Blumberg *et al.*, 1993). The only driver in the current model is the gauged Parker River discharge, which was obtained from the USGS gauging station at Byfield, Massachusetts, U.S.A. for the period during which salinity was measured (Figure 2). For the dye simulation, both $c_{Ld}(t)$ and $c_{Rd}(t)$ were set to zero and the dye plume was initialized around the release point as a Gaussian distribution such that 99·99% of the dye volume added would be located within ± 100 m of the release point at t_0. Concentration of state variables in lateral inputs, $\mathbf{c}_{li}(t)$, were all set to zero for both salt and dye simulations (they are included in Equation 1 for characteristic mixing-time calculations and for work currently being done on a nutrient limited food-web model).

The one-dimensional partial differential equation (Equation 1) was numerically integrated using a variable time step, moving grid routine (TOMS731) (Blom & Zegeling, 1994) obtained from netlib (URL http://www.netlib.org/). The simulation used to generate salinity distributions at each observation point was initialized on 6 April 1992 and ran until 12 April 1995 on a 30 node grid. The two dye plume simulations were run on a 100 node grid for the time period when dye measurements were taken. Parameters used in the model are given in Table 2).

Characteristic time scales of mixing

Characteristic time scales for mixing in an estuary are useful in determining whether or not a particular process (e.g. utilization of dissolved organic matter, toxicity effects of a pollutant, etc.) will be important within the estuary. Unfortunately, terminology pertaining to characteristic time scales of an element in a reservoir can be confusing due to different reference frames used for time, to different names that have

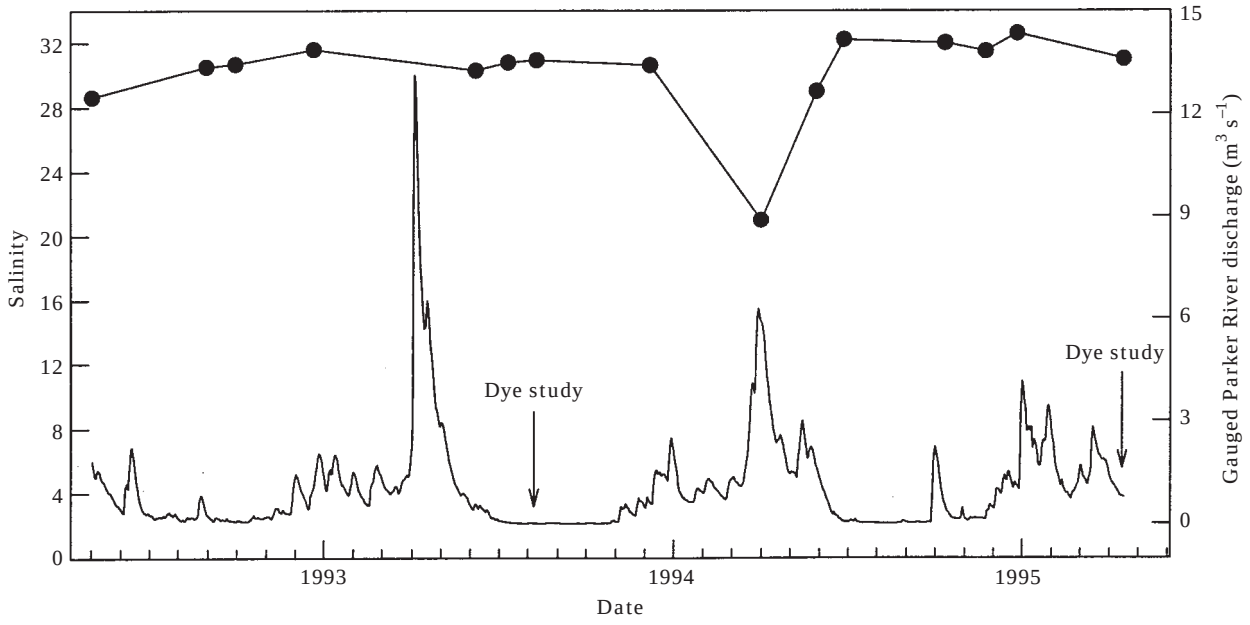

FIGURE 2. Off-shore salinity (line with filled circles) used for right boundary condition (Equation 11), and USGS gauged Parker River discharge at Byfield, Massachusetts, U.S.A., used to drive left boundary condition (Equation 10). The dates of the two dye release studies are also illustrated.

been defined for equivalent properties, to the extent to which inputs and geographical subsections of the estuary are distinguished, and to non-rigorous or improper use of definitions in the literature. In terms of time frames, the time a particle has spent in a reservoir can either be referenced to when it entered the reservoir, its age τ_a (Bolin & Rodhe, 1973), or the time remaining before it exits the reservoir, its residence (or remaining) time τ_r (Zimmerman, 1976). Another useful time scale refers to the time that it takes for an element to traverse the estuary, which is known as its transit time, τ_t. All three time scales can be averaged over the ensemble of particles in (or crossing the boundary of) an estuary to provide estimates of average age, $\langle\tau_a\rangle$, average residence time $\langle\tau_t\rangle$, and average transit time, $\langle\tau_t\rangle$ under steady-state conditions (Bolin & Rodhe, 1973; Zimmerman, 1976). Bolin and Rodhe's (1973) analogy with a human population is helpful in understanding the differences between these time scales: $\langle\tau_a\rangle$ is the average age of the population, while $\langle\tau_t\rangle$ is the average life expectancy of a newborn. The analogy is less applicable for $\langle\tau_r\rangle$, which is the average remaining life time for the entire population. It can be shown (Takeoka, 1984), that the average age equals the average residence time if sources and sinks are not distinguished, and only the whole estuary is considered (i.e. geographical subsections and point locations are not allowed). However, when these time scales are calculated for particular input sources (such as fresh water vs salt water) and/or particular locations within the estuary, equality need not exist between $\langle\tau_a\rangle$ and $\langle\tau_r\rangle$ (Zimmerman, 1976; Dronkers & Zimmerman, 1982). Since the general theory covering residence times has been previously developed (see Zimmerman, 1988, and references therein), we will only develop expressions for the averaged quantities for our one-dimensional estuary model described by Equations 1–4, 10 and 11.

Average age. We define $M(a, \Delta x; x, \tau_a)$ as the mass of material originating from input a (i.e. a river input or seawater) that lies within a subsection of the estuary between x and $x+\Delta x$ and has an age less than or equal to τ_a. If a tracer is introduced as a step function at input a and its concentration within the estuary, $c_t(a;x,\tau_a)$, is determined from Equation 1 as a function of distance and time since its addition, then $M(a,\Delta x;x,\tau_a)$ is given by:

$$M(\alpha,\Delta x;x,\tau_a) = \int_x^{x+\Delta x} c_t(\alpha;x,\tau_a)A(x)\,dx \qquad (12)$$

and the total mass of material originating from a between x and $x+\Delta x$ is given by:

$$M_0(\alpha,\Delta x;x) = \int_x^{x+\Delta x} c_t(\alpha;x,\infty)A(x)\,dx \qquad (13)$$

where $c_t(\alpha;x,\infty)$ is the steady-state concentration of the tracer. From these definitions, it can be shown (Zimmerman, 1976) that the average age of material between x and $x+\Delta x$ originating from α is given by:

$$\langle \tau_a(\alpha,\Delta x;x)\rangle = \int_0^\infty \left(1 - \frac{M(\alpha,\Delta x;x,t)}{M_0(\alpha,\Delta x;x)}\right) dt \qquad (14)$$

In the limit $\Delta x \to 0$, then:

$$\langle \tau_a(\alpha;x)\rangle = \int_0^\infty \left(1 - \frac{c_t(\alpha;x,t)}{c_t(\alpha;x,\infty)}\right) dt \qquad (15)$$

Hence, $\langle \tau_a(\alpha;x)\rangle$ at any location in the estuary can be calculated by following the concentration of the tracer at x with time.

Average residence time. Unlike the average age, the average residence time only depends on location in the estuary, not on the location of the source (Zimmerman, 1976). However, at times it is useful to examine the residence time of material within a specified subsection of the estuary; for instance, the average time is takes for an element originating in the upper estuary to leave the upper estuary (instead of the whole estuary). Consequently, we defined $M(\beta,x_{lb},x_{ub};\tau_r)$ as the mass of material in a subsection of the estuary between x_{lb} and x_{ub} that originated at β ($x_{lb} \le \beta \le x_{ub}$) and has a residence time less than or equal to τ_r. If a tracer is uniformly distributed at β within the estuary at τ_r zero, then $M(\beta, x_{lb},x_{ub};\tau_r)$ is given by:

$$M(\beta,x_{lb},x_{ub};\tau_r) = M_0(\beta) - \int_{x_{lb}}^{x_{ub}} c_t(\beta;x,\tau_r)A(x)\,dx, \qquad (16)$$

where $$M_0(\beta) = \int_{x_{lb}}^{x_{ub}} c_t(\beta;x,0)A(x)\,dx,$$

$c_t(\beta;x,\tau_r)$ is the concentration of the tracer, and the quantity $M_0(\beta)$ is the total mass of tracer initially released. From these definitions, it can be shown (Zimmerman, 1976) that the average residence time of material originating at β between x_{lb} and x_{ub}, $\langle \tau_r(\beta,x_{lb},x_{ub})\rangle$, is given by:

$$\langle \tau_r(\beta,x_{lb},x_{ub})\rangle = \int_0^\infty \frac{M(\beta,x_{lb},x_{ub};t)}{M_0(\beta)}\,dt \qquad (17)$$

Although β can be a point release (i.e. a Dirac delta function at x), this is difficult to implement numerically, so simulations were run in which the tracer was uniformly distributed over a broad area, such as the upper estuary.

Average transit time. The average transit time of an element originating from source α, $\langle \tau_t(\alpha)\rangle$, is the same as the turnover or flushing time (Zimmerman, 1976; Bolin & Rodhe, 1973) of this material. Consequently, if a tracer is added as a step function at α and allowed to attain a steady-state distribution in the estuary, $c_t(\alpha;x,\infty)$, then $\langle \tau_t(\alpha)\rangle$ is given by:

$$\langle \tau_t(\alpha)\rangle = \frac{1}{F(\alpha)} \int_R c_t(\alpha;x,\infty)A(x)\,dx \qquad (18)$$

where $F(\alpha)$ is the mass flux of tracer into the subregion R of the estuary. For fresh water, $F(\alpha)$ is given by $\Sigma_i q(\alpha;x_i)c_t(\alpha)$ where $c_t(\alpha)$ is the concentration of the tracer in the input and $q(\alpha;x_i)$ is the discharge rate of source i. Calculating $\langle \tau_t(\alpha)\rangle$ for saltwater inputs is problematic, since the flux of sea water into the estuary, $F(\alpha)$, depends on $D(x_R)A(x_R)/\ell$, where ℓ is an ambiguous length scale appropriate for dispersion at the mouth of the estuary (x_R). Consequently, $\langle \tau_t(\alpha)\rangle$ for seawater, or other oceanic materials transported by dispersion, is subject to interpretation if the transport flux is not directly measured (Park & James, 1989).

Characteristic mixing-time scales were calculated for the four estuarine subsections illustrated in Figure 1, as well as the whole estuary. The simulations used to generate tracer data were run on a 100 node grid with fixed freshwater discharge rates (q_{PR}) of 0·01, 0·1, 1·0 or 10·0 $m^3\,s^{-1}$. Third-degree interpolating polynomials were fit to the discrete numerical tracer data to facilitate numerical quadrature.

Results and discussion

Estimation of dispersion

From salinity. Typical salinity profiles at extreme low (0·008 $m^3\,s^{-1}$) and high (5·89 $m^3\,s^{-1}$) Parker River discharges, along with sigmoidal fits to the data from Equation 7, illustrate the strong influence of river discharge on salinity profiles [Figure 3(a)]. From these data, as well as data collected between 28 April 1992 and 12 April 1995, the dispersion coefficient as a function of distance was estimated from Equation 6 assuming steady state salinity distributions [Figure 3(b)]. The estimated dispersion coefficient has a strong hyperbolic relationship with distance, as has been observed or used by others (Hetling & O'Connell, 1966; Officer, 1978; Ridd *et al.*, 1990; Vörösmarty & Loder, 1994). The range of values at any given location indicates that $D(x,t)$ may be a function of discharge, which has also been observed (Officer, 1978). However, because freshwater discharge varies over several orders of magnitude during

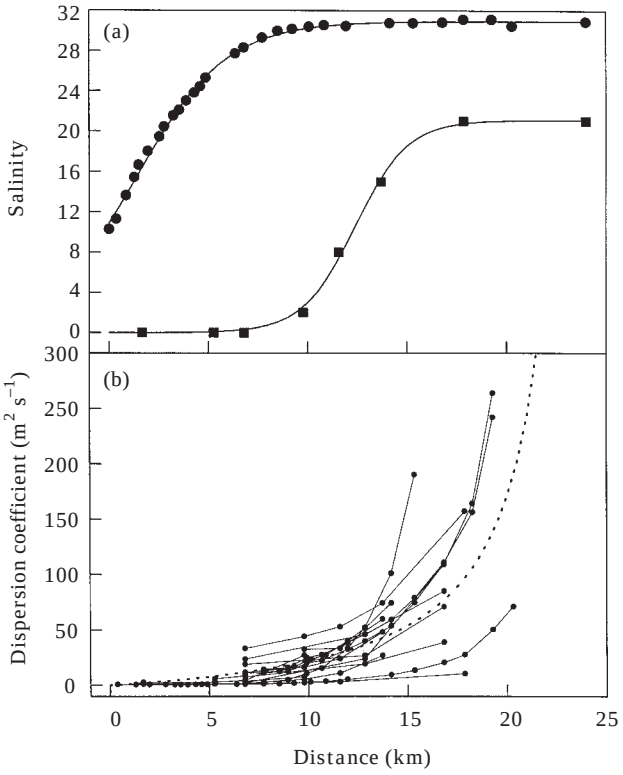

FIGURE 3. (a) Characteristic salinity distributions at high tide as a function of distance in the Plume Island Sound estuary during high (■, 5·89 m^3 s^{-1} on 28 March 1994) and low (●, 0·008 m^3 s^{-1} on 6 August 1993) Parker River discharge. Solid lines illustrate best fit of sigmoidal function (Equation 7) to salinity data. (b) Estimation of dispersion coefficient from 15 salinity transects (data illustrated in Figure 6) under steady-state assumption, Equation 6. Discrete estimates of the dispersion coefficient from the same salinity transect are connected by lines. The dotted line illustrates the dispersion coefficient given by Equation 20.

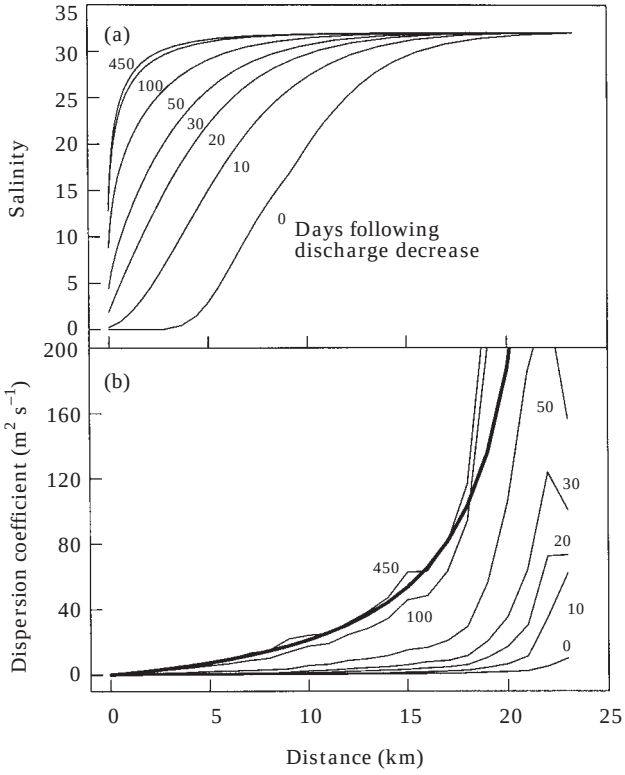

FIGURE 4. (a) Relaxation of a steady-state salinity distribution following a step down in Parker River discharge from 1·0 to 0·01 m^3 s^{-1}. Time following step down is given in days. (b) Estimated dispersion coefficient from salinity data given in (a) assuming steady state. Actual dispersion coefficient is illustrated by bold line.

the course of a year (Figure 2), it is possible that the variability in $D(x,t)$ at x could be due to inappropriate application of the steady-state assumption (Equation 6) for some salinity distributions (Ward & Fischer, 1971).

To investigate characteristic response times for salinity subject to changes in freshwater discharge, a simulation was run in which the Parker River discharge, $q_{PR}(t)$, was held at 1·0 m^3 s^{-1} until steady state was obtained, then stepped down to 0·01 m^3 s^{-1}. Salinity distributions during the transient period [Figure 4(a)] were used in conjunction with Equations 6 and 7 to estimate the dispersion coefficient as a function of distance from the dam at various times [Figure 4(b)]. Salinity distributions will rapidly approach steady state under high discharge conditions (greater than 1 m^3 s^{-1}), but under low flow conditions distributions can take up to 3 months to reach steady state [Figure 4(a)]. During this transient period, estimates of dispersion based on salinity will be in gross error if the system is assumed to be at steady state [Figure 4(b)]. The transient nature of the system presents a difficulty for estimating the dispersion coefficient in the upper reaches of the Parker River, because Equation 6 is best applied in those areas of the estuary where $dc_s(x)/dx$ is significantly different from zero. However, a significant salinity gradient in the upper Parker only occurs at low freshwater discharge, when the applicability of the steady-state assumption is most dubious.

From dye studies. In order to obtain a better estimate for the dispersion coefficient in the upper Parker River, two dye release studies were conducted under extreme low [Figure 5(a)] and average [Figure 5(b)] runoff conditions. For each observed tidal cycle following the dye release, an estimate of the dispersion coefficient near the dye release site was determined from a least squares fit of Equation 8 to the dye

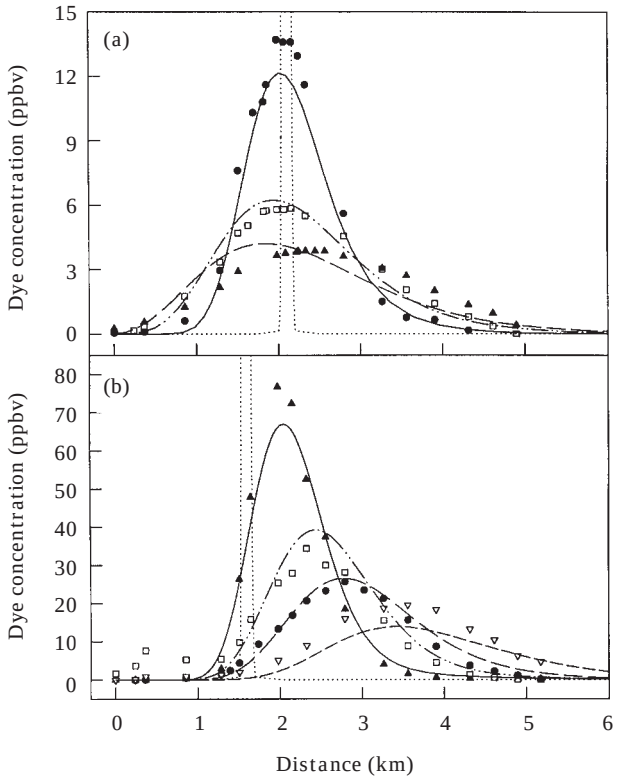

FIGURE 5. Dispersion of Rodamine Wt dye plume measured at high tide (symbols) following release of (a) 1·6 ℓ on 4 August 1993 and (b) 7·7 ℓ on 10 April 1995 in upper Parker River (at about 1·7 km) during extreme low (0·008 $m^3 s^{-1}$) and average (0·8 $m^3 s^{-1}$) Parker River discharges, respectively. Transient model (Equation 1) simulations for observed tidal cycles (lines) were run with the dispersion coefficient given by Equation 20 and a dye decomposition rate, k_d, of 0·14 $days^{-1}$. (a) ●, cycle 1; □, cycle 3; ▲, cycle 5. (b) ▲, cycle 1; □, cycle 2; ●, cycle 3; ▽, cycle 5. · · · model: cycle 0 (a and b); —— model: cycle 1 (a and b); – · · – model: cycle 3 (a)/2 (b); — – model: cycle 5 (a)/3 (b); – – – model: cycle 5 (b).

distribution. This analysis also provided an estimate for the dye decomposition coefficient, k_d, at each tidal cycle. Although the least-squares estimate of the dispersion coefficient for a particular tidal cycle is independent of the observations made at the other tidal cycles, both experiments produced consistent estimates of $D(x,t)$ over time (Table 3) (least-squares fits not shown). The observed dispersion coefficients are quite similar to the predicted values of 3·0 and 8·7 $m^2 s^{-1}$ given by Fischer *et al.* (1979) equations 5·19 and 7·2, respectively, assuming a tidal excursion of 4 km ($\bar{u}$ = 0·18 m s^{-1}); *W* (width), 15 m; *d* (depth), 1·5 m; *T* (period), 12·25 h; *u** (shear velocity) = 0·1 $\bar{u}$, and ε_t (transverse mixing) = 0·6 *du**. Interestingly, estimates for the dispersion coefficient at extreme low and average discharge rates (Table 3) did not differ

TABLE 3. Estimations of dispersion [$D(x,t)$] and dye decomposition (k_d) coefficients from dye release studies begun on 4 August 1993 (q_{PR} = 0·008–0·013 $m^3 s^{-1}$) and 10 April 1995 (q_{PR} = 0·76–0·96 $m^3 s^{-1}$)

Study I: August 1993			Study II: April 1995		
Tidal cycle	$D(x,t)$ ($m^2 s^{-1}$)	k_d (day^{-1})	Tidal cycle	$D(x,t)$ ($m^2 s^{-1}$)	k_d (day^{-1})
1	3·06	−0·15	1	1·90	0·12
3	3·12	0·12	2	2·60	0·39
5	3·12	0·11	3	2·02	0·24
			5	2·02	0·10

Estimates for $D(x,t)$ and k_d for each high tide observation (tidal cycle) were obtained from least-squares fit of Equation 8 to the dye plumes (Figure 5) (numerical fits not illustrated in figure).

significantly, even though the freshwater discharge differed by two orders of magnitude (0·008 *vs* 0·8 $m^3 s^{-1}$) between the two experiments. This indicates that $D(x,t)$ may not be as strong a function of discharge as suggested by the estimates obtained from the salinity profiles [Figure 3(b)], and implies that the steady-state assumption (Equation 6) may be inappropriate for some salinity distributions (i.e. those measured during low or rapidly changing discharge).

From parameter estimation. To avoid problems associated with estimating $D(x,t)$ from salinity data that have not attained steady-state distribution (i.e. Equation 6), the full transient model (Equation 1) was used to generate non steady-state salinity distributions. The following equation:

$$D(x,t) = D_M q(x,t)^n \left(\frac{x}{x_M - x} \right)^m + D_{MO} \qquad (19)$$

was used to represent the dispersion coefficient and its possible dependence on flow-rate. The adjustable parameters D_M, *n*, *m*, x_M, and D_{MO}, were determined by minimizing the squared error between the observed and predicted salinity profiles and the observed and predicted dispersion coefficient at the dye release site (Equation 9) with D_{dye} = 2·5 $m^2 s^{-1}$ and x_{dye} = 2000 m) via the technique previously described in the Modeling section. The best fits to the salinity data (Figure 6) and dye plumes (Figure 5) were obtained with the following expression for $D(x,t)$ ($m^2 s^{-1}$):

$$D(x,t) = 31{\cdot}42 \left(\frac{x}{24008 - x} \right)^{1{\cdot}055} \qquad (20)$$

where *x* is distance from the Parker dam in meters. Although dependence on freshwater discharge was

included in the general model for $D(x,t)$, Equation 19, the exponent, n, returned by the minimization routine was effectively zero, so as to render the dependency insignificant (same is true for D_{MO}). Consequently, it appears that the variability in $D(x,t)$ that was directly estimated from salinity profiles is due to the inappropriate application of the steady-state assumption rather than true dependence on flow rate [Figure 3(b)]. Without the information provided by the dye studies, a different conclusion might have been reached. If the parameter estimation routine is run without the constraints imposed by the dye study, then Equation 19 retains its dependence on flow-rate ($n \approx 0{\cdot}22$), but the model fit to the transient salinity data is not improved (data not shown). It is perhaps not surprising that the dispersion coefficient is not dependent on freshwater discharge, as it is likely that tidal dispersion is governed by tidal shear generated from Stokes' drift and compensation flow that are not strongly dependent on freshwater input (Feng *et al.*, 1986*b*; Dortch *et al.*, 1992).

The functionality determined for the dispersion coefficient, Equation 20, produces reasonable agreement between model predictions and observed salinity (Figure 6) and dye (Figure 5) distributions for freshwater discharges ranging from 0·008 to 5·9 $m^3 s^{-1}$. Our estimate of the dispersion coefficient (Equation 20) is of the same order of magnitude and spatial functionality as that used by Vörösmarty and Loder (1994) for the Parker River at a discharge of 0·3 $m^3 s^{-1}$. However, they assumed, based on data from other estuaries, that dispersion is dependent on freshwater discharge, which does not appear to be warranted for the Parker River estuary. With an accurate estimation of dispersion, the model can be reliably used to investigate characteristic mixing-time scales.

Characteristic time scales for transport

Average age. Average ages of freshwater and saltwater parcels, $\langle \tau_a(\alpha,\Delta x;x) \rangle$, in the four subsections and whole estuary (Figure 1), were calculated under four different freshwater discharge regimes from Equations 12–14 (Table 4). For these calculations, a tracer was added to either all freshwater inputs or to seawater. An example simulation for tracer added at unit concentration (1 mass m^{-3}) to all freshwater inputs under average discharge (1 $m^3 s^{-1}$) is illustrated in Figure 7(a). The tracer concentration is initially zero, but builds to a steady-state distribution over time [Figure 7(a)]. Although all lateral inputs are labeled with tracer, only Cart Creek (q_1 at 4·2 km) and Mill River (q_2 at 9·3 km) introduce observable perturbations in the tracer distributions [Figure 7(a)]. From this data, the total mass of the tracer at time t in a defined section of the estuary (say the upper Parker) is calculated from Equation 12, which is then used to construct an age distribution (AD) function [Figure 7(b)]. The integration of the AD function (i.e. Equation 14) provides the average age of material in the upper Parker River that originated from all freshwater inputs (for this example).

Average ages of fresh water are highly dependent on discharge, with the greatest dependency occurring in the upper Parker where the average age of fresh water can vary from about one month (for $q_{PR} = 0{\cdot}01$ $m^3 s^{-1}$) to less than a day (for $q_{PR} = 10{\cdot}0$ $m^3 s^{-1}$) (Table 4). The average freshwater age also exhibits a spatial maximum for a given discharge, with the mid section having the longest average age under low flows (Table 4, underlined entries). The maximum progresses towards the sound as flow-rate increases. On the contrary, the average age of salt water depends more on location than on discharge, which is largely due to the single location of saltwater input. For instance, the average age of salt water in the sound is approximately 1 day, independent of discharge (Table 4, lower half).

Average residence time. Average residence times, $\langle \tau_r(\beta,x_{lb},x_{ub}) \rangle$, of a water parcel originating at β within the whole estuary ($x_L \le x \le x_R$) or estuarine subsection ($x_{lb} \le x \le x_{ub}$) were calculated from Equations 16 and 17 for four different discharge rates (Table 5). For these calculations, a particular section of the estuary was uniformly labeled with a tracer (β), and its concentration within an estuarine section ($x_{lb} \le x \le x_{ub}$) was followed over time. An example simulation is illustrated in Figure 7(c), in which the upper Parker is labeled. The total mass of tracer in either the upper Parker or in the whole estuary was determined from Equation 16 in order to generate residence time distribution (RTD) functions for either the upper Parker or the whole estuary [Figure 7(d)]. These functions were then integrated (Equation 17) to give the average residence time of water originating in the upper Parker remaining in either the upper Parker or the whole estuary (for this example).

The average residence times of water in a subsection, remaining in that subsection, display strong dependence on discharge (Table 5, upper half), similar to the average ages calculated above. Average residence times also exhibit a maximum for a given discharge (Table 5, underlined entries). Maxima occur because the upper Parker is dominated by advection at average to high flows, while the lower Parker and sound are dominated by strong dispersive

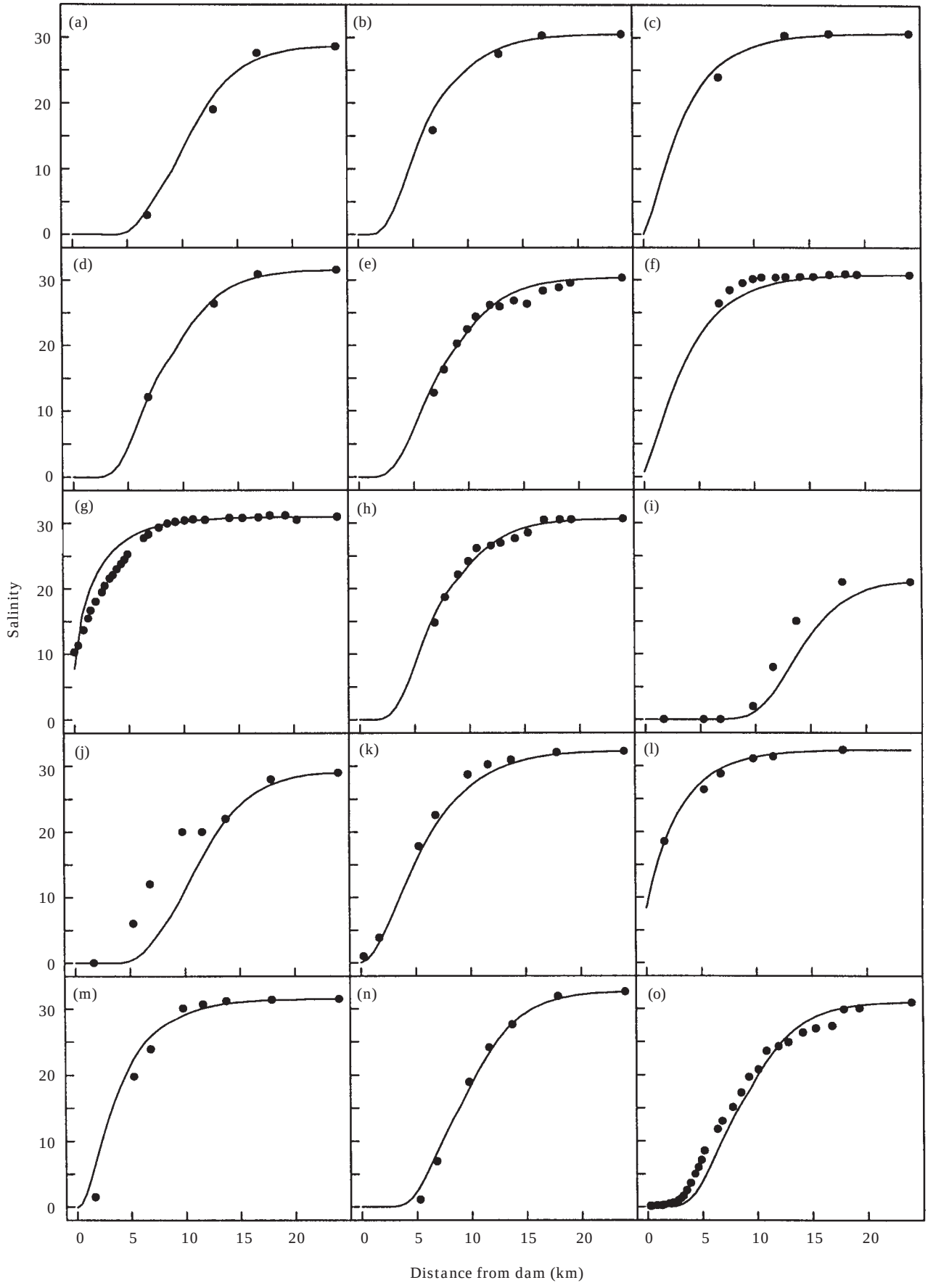
(a)
(b)
(c)
(d)
(e)
(f)
(g)
(h)
(i)
(j)
(k)
(l)
(m)
(n)
(o)
Salinity
0
10
20
30
0
5
10
15
20
Distance from dam (km)

TABLE 4. Average ages $\langle \tau_a(a,\Delta x;x)\rangle$ of fresh water (upper half of table) and salt water (lower half) in the four subsections and entire estuary under four different Parker River gauged discharges

Discharge q_{PR} ($m^3\ s^{-1}$)	Upper	Mid	Lower	Sound	Whole Estuary
Average age (days) of fresh water					
0·01	27·2	35·1	28·9	25·5	28·9
0·1	15·8	23·6	20·8	18·8	19·1
1·0	3·32	8·78	9·84	9·11	8·23
10	0·31	1·14	2·26	3·20	2·42
Average age (days) of salt water					
0·01	33·8	17·3	7·94	1·37	3·17
0·1	25·6	15·5	7·40	1·14	2·57
1·0	13·7	10·2	5·60	0·88	1·51
10	—[a]	3·68	2·44	0·47	0·51

Underlined values indicate maximum for given discharge. Tracer concentration too low to calculate average age.

terms for all flows. Consequently, under low flow-rate, the upper Parker has the longest residence time, but as discharge increases the upper Parker is flushed quickly which results in a shorter average residence time than the mid Parker. Not surprisingly, average residence times of water originating in an estuarine subsection within the whole estuary (Table 5, lower half) are longer than the average residence times within that subsection (Table 5, upper half). Similar values between average ages of saltwater (Table 4, lower half) and average residence times in the whole estuary (Table 5, lower half) indicate that the input of salt water to the estuary is much greater than freshwater input, even under high runoff. As stated before, average age equals average residence time when inputs to the estuary are not distinguished (i.e. fresh water and salt water treated as a single input). If saltwater input is much greater than freshwater input, then the average age of a saltwater parcel will approach the average age of an 'unlabeled' water parcel and, hence, the average residence time of the water parcel. The equality will be exactly satisfied as freshwater input goes to zero, or saltwater input goes to infinity.

Average transit time. Average transit times, $\langle \tau_t(a)\rangle$, (also called turnover or flushing times) were calculated for each of the seven freshwater inputs, as well as the saltwater input, from Equation 18 (Table 6). These data represent the average time it takes for a water parcel originating from a specified input to exit the estuary entirely. For these calculations, a tracer at unit concentration was added to an input, and its steady-state distribution was determined. An example simulation for the Mill River input at average discharge is illustrated in Figure 7(e). The steady-state tracer distribution associated with the Mill River is integrated, Equation 18, to determine the total mass of tracer in the estuary: $0{\cdot}659 \times 10^6$ mass units [plateau in curve of Figure 7(f)]. This value is then divided by the mass flux of tracer into the estuary, $F(a) = q_2 C_{12} = (86\,400 \times 0{\cdot}875\ m^3\ day^{-1})$ (1·0 mass units m^{-3}), to give the average transit time of material entering the estuary from the Mill River under average discharge (for this example). Transient data [Figure 7(e,f)] are not used in the calculations; they only serve to indicate when steady state has been achieved.

The average transit times for the seven freshwater inputs under different discharge rates show considerable variation (Table 6). Inputs feeding the upper sections of the estuary exhibit significant dependence on discharge, while those closer to the mouth of the estuary are almost independent of discharge. Material entering the estuary via the Parker dam (q_0) can take on average as long as 55 days to leave the estuary, while Ipswich River water (q_6) exits the estuary almost immediately (Table 6). Even though the Ipswich

FIGURE 6. Comparison between observed and estimated salinity distributions. Simulations were run with dispersion coefficient given by Equation 20. Salinity transects were conducted at high tide on (a) 28 April 1992, (b) 26 August 1992, (c) 25 September 1992, (d) 16 December 1992, (e) 3 June 1993, (f) 7 July 1993, (g) 6 August 1993, (h) 2 December 1993, (i) 28 March 1994, (j) 25 May 1994, (k) 23 June 1994, (l) 25 July 1994, (m) 18 November 1994, (n) 21 December 1994, and (o) 12 April 1995. Salinities measured at the mouth of Plume Island Sound on the above dates provide the right boundary condition as illustrated in Figure 2. Salinity data for Figures (a)–(f) and (h) were obtained from Rines *et al.* (1994).

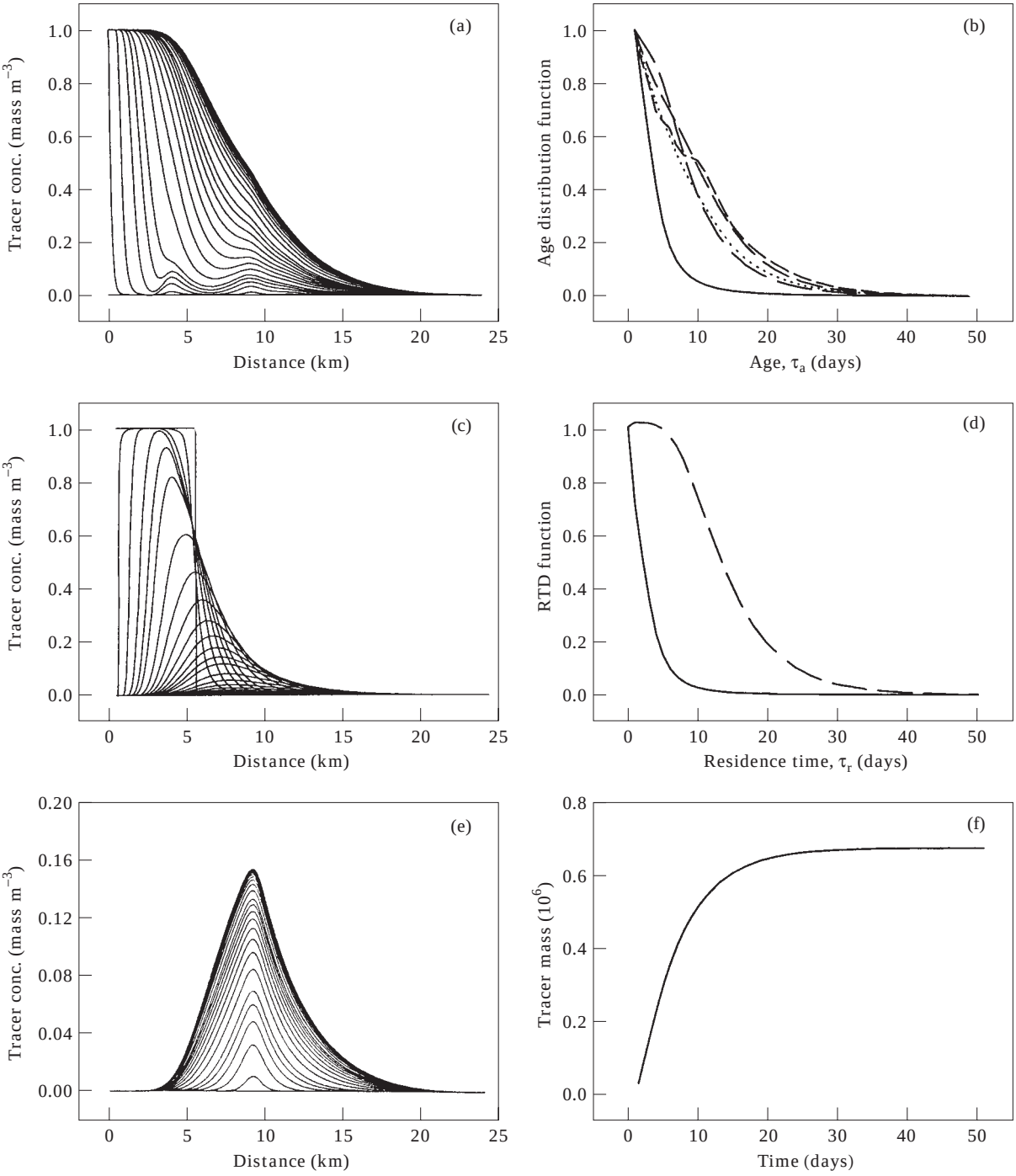

FIGURE 7. Examples of tracer simulations to estimate characteristic time scales for transport. (a) Transient concentrations following tracer addition of unit concentration to all freshwater inputs. (b) Age distribution function (integrand of Equation 14) calculated from (a) for the four estuarine subsections and whole estuary. (c) Transient tracer concentration following the uniform labeling of the upper Parker River. (d) Residence time distribution function (RTD: integrand of Equation 17) calculated from (c) for the upper Parker and whole estuary. (e) Transient tracer concentration following labeling of Mill River input (q_2). (f) Total mass of tracer in whole estuary as a function of time calculated from (e). (b): —— upper Parker; — – mid Parker; — — lower Parker; – – – Sound; · · · whole estuary, (d) —— in upper Parker; — — in whole estuary.

TABLE 5. Average residence times, $\langle \tau_r(\beta, x_{lb}, x_{ub}) \rangle$, of water in a subsection remaining within that subsection (upper half of table), or within the whole estuary (lower half)

Discharge q_{PR} ($m^3 s^{-1}$)	Upper	Mid	Lower	Sound	Whole Estuary
Average residence time (days) in subsection					
0·01	18·1	6·83	3·83	0·79	
0·1	11·9	6·42	3·69	0·72	
1·0	2·8	4·00	3·13	0·69	
10	0·30	0·63	1·18	0·58	
Average residence time (days) in whole estuary					
0·01	34·3	17·3	7·84	1·22	3·24
0·1	27·6	15·6	7·47	1·10	3·00
1·0	14·9	10·5	5·76	0·97	2·18
10	4·99	4·11	2·71	0·63	1·07

Underlined values indicate maximum for given discharge.

TABLE 6. Average transit times (days) for water originating from one or more lateral inputs or the sea to the mouth of Plume Island Sound estuary

Input source	Parker gauged discharge ($m^3 s^{-1}$)			
	0·01	0·1	1·0	10·0
Parker River Dam (q_0)	54·8	38·0	17·2	5·02
Cart Creek (q_1)	28·3	24·2	14·1	4·62
Mill River (q_2)	12·8	11·9	8·72	3·56
Little River (q_3)	8·23	7·92	6·18	2·88
Mud Creek + Plum Island River (q_4)	3·67	3·87	3·28	1·85
Rowley + Roger Island + Eagle Hill Rivers (q_5)	1·12	1·16	1·04	0·69
Ipswich River (q_6)	0·05	0·06	0·05	0·04
All freshwater inputs	8·08	6·08	3·25	1·15
Salt water	0·63[a]	0·62[a]	0·58[a]	0·46[a]
	4190[b]	413[b]	38·7[b]	3·0[b]

[a]Estimated from tidal prism volume (lower bound).
[b]Estimated from advective flux (upper bound).

River input is almost seven times greater than the Parker dam discharge (Table 1), its impact on the estuary is much smaller because it is quickly diluted with offshore water. A note of caution is added here, however. Although our surveys indicate that the Plum Island Sound estuary is fairly well mixed, there exists significant hydrodynamic structure due to estuarine residual circulation (Feng *et al.*, 1986*b*), such as Stokes' drift and compensation flow as previously discussed. Consequently, it is possible that a non-negligible amount of Ipswich River water could be advected to the upper reaches of the Sound before complete lateral mixing occurred, which would result in longer times and larger spatial scales of transport than estimated here. Investigation of such phenomena requires explicit hydrodynamic models and more extensive surveys (Dortch *et al.*, 1992; Signell & Butman, 1992), but this is beyond the intent of this initial analysis of the Plum Island Sound estuary.

Average transit time for saltwater input is a more dubious calculation. Although the mass of tracer in the estuary associated with saltwater input can be easily determined (integral part of Equation 18), the mass flux, $F(a)$, due to dispersive and advective transport is difficult to estimate (Zimmerman, 1988). One way to estimate $F(a)$ is to assume that each flood tide is completely mixed with the estuarine water (Zimmerman, 1988), which would imply $F(a)$ equals $\sim 2V_{tp}$ per day, where V_{tp} is the average tidal prism volume (32 Mm^3). This gives an average transit time of approximate 0·5 days (Table 6), which represents a lower bound. Another technique for estimating $F(a)$ is to assume it equals $D(x_R)A(x_R)/\ell$), where the characteristic length scale for transport, ℓ, is the tidal

excursion at the estuarine mouth, which is greater than 14 km for the Plum Island Sound estuary. From Equations 3 and 20, this produces a mass transport of 3800 $Mm^3\ day^{-1}$ at x_R (24 km) and $\ell = 20$ km, which is 100 times greater than the tidal prism estimate. This unreasonably large estimate for $F(a)$ is caused by the hyperbolic equation used to represent $D(x)$, Equation 20. Since this equation has a singularity at $x = 24\,008$, the estimate for $D(x)$ becomes extremely large at the mouth of the estuary. Consequently, estimating $F(a)$ from $D(x)$ is not reliable for this case. A lower bound on $F(a)$ is given by $q(x_R)c_t(x_R,\infty)$, since the advective transport of tracer out of the estuary must equal the net dispersive transport of tracer into the estuary. Clearly this produces an upper bound on $\langle\tau_t(a)\rangle$, since as freshwater input goes to zero, average transit time of salt water goes to infinity. Nevertheless, these upper bounds on $\langle\tau_t(a)\rangle$ for salt water are also given in Table 6.

Average transit times (flushing times) were calculated for various subsections of the Plum Island Sound estuary as part of the MiniBays study (Rines *et al.*, 1994). Average transit times of fresh water in that study were calculated using a box model approach, coupled to salinity measurements and freshwater inputs. Although a direct comparison between results can not be made due to differences in compartmentalization inherent in the box model approach, they obtained average transit times on the order of a few days for the combined Parker River–Plum Island Sound system, which are similar to our results for all freshwater inputs (Table 6).

Ecological importance

The three characteristic mixing-time scales calculated above have different applicability to ecological processes that occur in the estuary. Some of the questions of interest include the extrapolation of results obtained from *in vitro* incubations to *in situ* processing in the estuary, the likelihood of an estuarine subsection to support a phytoplankton bloom, the fate of pollutants, and the fraction of material transported into the estuary from freshwater and saltwater sources that is processed within the estuary. The relevance between these processes and the three time scales are discussed below.

Average age of a water parcel is useful when considering decomposition processes. Consider, for example, organic matter derived from terrestrial inputs (i.e. associated with freshwater inputs). If a water sample was taken at a particular location within the estuary, its age since entering the estuary would depend on discharge (and location). Organic matter sampled in the upper Parker during high discharge would be relatively fresh (less than one day, see Table 4). An *in vitro* incubation of this water would likely indicate a significant fraction of easily utilized material. On the contrary, under extreme low flow conditions that often exist in the summer months (Figure 2), organic matter derived from freshwater inputs would be approximately one month old throughout the estuary (Table 4), so a similar incubation would likely indicate fairly refractory material.

Average residence times were calculated for both the whole estuary and subsections because both are ecologically important (Table 5). Average residence time within a subsection is an important time scale for growth of plankton within that subsection because if the plankton's doubling time is longer than the residence time of the section, then the plankton will most likely be washed out of the estuarine section. For instance, under high flow rate ($10\ m^3\ s^{-1}$) plankton in the upper Parker would have an average residence time of only 0·3 days within that section, but 5 days within the entire estuary (Table 5). Consequently, assuming a specific growth rate of 2 $days^{-1}$ for phytoplankton (Eppley, 1972), we would not expect to find a bloom in the upper Parker under these conditions, but we might expect to find a bloom somewhere down stream since it takes 5 days on average for the water mass to leave the estuary entirely. Indeed, this is what has been observed in the Plum Island Sound estuary (Wright *et al.*, 1987). In Spring when discharge is high (Figure 2), phytoplankton blooms occur in the lower Parker River and Sound, but when discharge is low, as occurs in the summer months, the phytoplankton bloom is found in the upper and mid sections of the Parker River (Wright *et al.*, 1987). Average residence time of a water mass in the whole estuary is also an important time scale for flushing of pollutants. For these types of events, one is usually most interested in the time it will take to remove the pollutant from the estuary entirely, not just the subsection of the estuary where the pollutant was introduced. Hence, the appropriate spatial scale depends on the question(s) being asked. Complimentary to average age, average residence time is also important for incubation studies. If an incubation of a water sample indicates that a compound has a half-life of 10 days, but the residence time of the water parcel is 1 day, then most of the compound will be transported out of the estuary before a significant fraction has reacted.

Average transit time is useful in determining the fraction of material in a particular input that is likely to be processed within the estuary. It is useful for

calculating overall budgets and the likely impacts of pollutants associated with an input. For example, under extreme low flow, material associated with the Parker dam input will take an average of 55 days to exit the estuary. Compounds with a lability less than 55 days are likely to be utilized within the estuary. On the contrary, the majority of material associated with the Ipswich River will be passed to the coastal shelf, since the average transit time of this water is only slightly greater than an hour (Table 6). Although average transit times (or flushing times) are often reported to indicate how quickly a system will be flushed, they can be misleading. Consider a bay which has a high mass exchange with the ocean. In this case, the average transit time will be short; however, it is likely that most of the material that is transported into the bay will be immediately transport out, leaving the material already in the bay relatively unaffected (e.g. the upper Parker River *vs* the sound). Consequently, a phytoplankton bloom in the bay supported by high nutrient concentrations in low freshwater runoff would not be readily washed out of the bay, even though the average transit time is short. Hence, distinguishing different time scales, geographical subsections and water inputs is necessary to adequately characterize an estuary.

Summary

We have demonstrated how salinity data, dye studies, and parameter estimation techniques can be used to obtain accurate estimates of dispersion as a function of distance in the Plum Island Sound estuary. Although the salinity data, in conjunction with the steady-state assumption, indicates that the dispersion coefficient may be a function of freshwater discharge, the dye release studies do not support this dependence on discharge. However, the two observations are not contradictory, because use of salinity data that is not at steady state will produce variability in the estimated dispersion coefficient that resembles flow dependence (Figure 4). Indeed, we were able to obtain good predictions for both the salinity profile (Figure 6) and the dye dispersion (Figure 5) without requiring flow dependence on the dispersion coefficient (Equation 20) if the steady state approximation was not invoked. The dye studies were especially useful in determining the value of the dispersion coefficient in the upper section of the estuary (Table 3) where salinity gradients significantly different from zero almost never occur under steady-state conditions due to the long relaxation time that is inherent under low flow conditions (Figure 4).

With an accurate description of the dispersion coefficient (Equation 20), characteristic time scales involving average age (Table 4), residence time (Table 5) and transit time (Table 6) for various inputs and locations within the Plum Island Sound estuary were calculated. Although there is often a tendency to calculate a single characteristic time scale for the entire estuary (such as the average transit time of the fresh water), it is clear that many time scales exist, and they are dependent on discharge and location within the estuary. Furthermore, the most appropriate time scale, average age, residence time or transit time, depends on the question(s) being addressed.

Acknowledgements

We gratefully thank Hap Garritt, Ishi Buffam, Katherine Bowman, Krista Ingram, Derrick Alderman, and Brian Balsis for their assistance in the dye release experiments and the salinity transect surveys, and John Kim for the site map. This work was supported by the National Science Foundation Land Margin Ecosystem Research program (OCE-9214461), the Sweetwater Trust, and the Lakian Foundation.

References

Blom, J. G. & Zegeling, P. A. 1994 Algorithm 731: a moving-grid interface for systems of one-dimensional time-dependent partial differential equations. *Association for Computing Machinery Transactions on Mathematical Software* **20,** 194–214.

Blumberg, A., Signell, R. & Jenter, H. 1993 Modeling transport processes in the coastal ocean. *Journal of Marine Environmental Engineering* **1,** 31–52.

Blumberg, A. F. & Kantha, L. H. 1985 Open boundary condition for circulation models. *American Society of Civil Engineers Journal of Hydraulic Engineering* **111,** 237–255.

Bolin, R. & Rodhe, H. 1973 A note on the concepts of age distribution and transit time in natural reservoirs. *Tellus* **25,** 58–62.

Box, M. J. 1966 A comparison of several current optimization methods, and the use of transformations in constrained problems. *Computer Journal* **9,** 67–77.

Brent, R. P. 1973 *Algorithms for Minimization Without Derivatives*. Prentice-Hall, New Jersey, 195 pp.

Chatwin, P. C. & Allen, C. M. 1985 Mathematical models of dispersion in rivers and estuaries. *Annual Review of Fluid Mechanics* **17,** 119–149.

Dortch, M. S., Chapman, R. S. & Abt, S. R. 1992 Application of three-dimensional Lagrangian residual transport. *Journal of Hydraulic Engineering* **118,** 831–848.

Dronkers, J. 1982 Conditions for gradient-type dispersive transport in one-dimensional, tidally averaged transport models. *Estuarine, Coastal and Shelf Science* **14,** 599–621.

Dronkers, J. & Zimmerman, J. T. F. 1982 Some principles of mixing in tidal lagoons. *Oceanologica Acta* **SP,** 107–117.

Dyer, K. R. 1974 The salt balance in stratified estuaries. *Estuarine and Coastal Marine Science* **2,** 273–281.

Eppley, R. W. 1972 Temperature and phytoplankton growth in the sea. *Fishery Bulletin* **70,** 1063–1085.

Feng, S., Cheng, R. T. & Xi, P. 1986*a* On tide-induced Lagrangian residual current and residual transport. 1. Lagrangian residual current. *Water Resources Research* **22,** 1623–1634.

Feng, S., Cheng, R. T. & Xi, P. 1986*b* On tide-induced Lagrangian residual current and residual transport. 2. Residual transport with application in South San Francisco Bay, California. *Water Resources Research* **22,** 1635–1646.

Fenneman, N. M. 1938 *Physiography of the Eastern United States*. McGraw Hill, New York, 714 pp.

Fischer, H. 1976 Mixing and dispersion in estuaries. *Annual Review of Fluid Mechanics* **8,** 107–133.

Fischer, H. B., List, E. J., Koh, R. C. Y., Imberger, J. & Brooks, N. 1979 *Mixing in Inland and Coastal Waters*. Academic Press, New York, 483 pp.

Geyer, W. R. & Signell, R. P. 1992 A reassessment of the role of tidal dispersion in estuaries and bays. *Estuaries* **15,** 97–108.

Gunn, D. J. & Yenigun, O. 1985 Estimation of dispersion in estuaries by a self-consistent method. *Estuarine, Coastal and Shelf Science* **21,** 257–272.

Guymer, I. & West, J. R. 1992 Longitudinal dispersion coefficients in estuary. *American Society of Civil Engineers Journal of Hydraulic Engineering* **118,** 718–734.

Hansen, D. V. & Rattray, M. 1966 New dimensions in estuary classification. *Limnology and Oceanography* **11,** 319–325.

Hetling, L. J. & O'Connell, R. L. 1966 A study of tidal dispersion in the Potomac River. *Water Resources Research* **2,** 825–841.

Hopkinson, Jr. C. & Vallino, J. J. 1995 The relationships among man's activities in watersheds and estuaries: a model of runoff effects on patterns of estuarine community metabolism. *Estuaries* **18,** 598–621.

Ketchum, B. 1951 The dispersion and fate of pollution discharged into tidal waters, and the viability of enteric bacteria in the area. Woods Hole Oceanographic Institution, Woods Hole, WHOI51-11, 16 pp.

Longuet-Higgins, M. S. 1969 On the transport of mass by time-varying ocean currents. *Deep-Sea Research* **16,** 431–447.

Miller, R. L., Bradford, W. L. & Peters, N. E. 1988 Specific conductance: theoretical considerations and application to analytical quality control. *USGS Water-Supply Paper*, Denver, **2311,** 16 pp.

Officer, C. B. 1978 Some simplified tidal mixing and circulation flux effects in estuaries. In *Estuarine Transport Processes* (Kjerfve, B., ed.). University of South Carolina Press, Columbia, pp. 75–93.

Park, J. K. & James, A. 1989 A unified method of estimating longitudinal dispersion in estuaries. *Water Science and Technology* **21,** 981–993.

Ridd, P. V., Wolanski, E. & Mazda, Y. 1990 Longitudinal diffusion in mangrove-fringed tidal creeks. *Estuarine, Coastal and Shelf Science* **31,** 541–554.

Rines, H. M., Turner, A. C., Galagan, C. & Mendelsohn, D. L. 1994 *Water Quality Surveys and Flushing Characteristics of the Plum Island Sound/Rivers system*. Massachusetts Audubon Society: North Shore, Wareham, 102 pp.

Sammel, E. A. 1967 Water resources of the Parker and Rowley River basins Massachusetts. *U.S. Geological Survey, Hydrologic Investigations*, Washington, D.C., HA-247, 9 pp.

Signell, R. P. & Butman, B. 1992 Modeling tidal exchange and dispersion in Boston Harbor. *Journal of Geophysical Research* **97,** 15591–15606.

Smith, R. 1977 Long-term dispersion of contaminants in small estuaries. *Journal of Fluid Mechanics* **82,** 129–146.

Takeoka, H. 1984 Fundamental concepts of exchange and transport time scales in a coastal sea. *Continental Shelf Research* **3,** 311–326.

Vörösmarty, C. J. & Loder, T. C. 1994 Spring-neap tidal contrasts and nutrient dynamics in a marsh-dominated estuary. *Estuaries* **17,** 537–551.

Ward, P. R. B. & Fischer, H. B. 1971 Some limitations on use of the one-dimensional dispersion equation, with comments on two papers by R. W. Paulson. *Water Resources Research* **7,** 215–220.

Wright, R. T., Coffin, R. B. & Lebo, M. E. 1987 Dynamics of planktonic bacteria and heterotrophic microflagellates in the Parker Estuary, northern Massachusetts. *Continental Shelf Research* **7,** 1383–1397.

Zimmerman, J. T. F. 1976 Mixing and flushing of tidal embayments in the western Dutch Wadden Sea, Part I: distribution of salinity and calculation of mixing times. *Netherlands Journal of Sea Research* **10,** 149–191.

Zimmerman, J. T. F. 1988 Estuarine residence times: Volume I Estuarine physics. In *Hydrodynamics of Estuaries* (Kjerfve, B., ed.). CRC Press, Boca Raton, pp. 75–84.